> 0), the signs +, −, +, and − are observed for the *B* terms for the L_b, L_a, B_b, and B_a transitions. The observed MCD signs are well reproduced also by the LCOAO calculation (Figure 4; Table II). The *B* terms predicted by LCOAO for the strong B_b and B_a transitions (bands 3 and 4) are the result of magnetic coupling between several near-degenerate transitions, as discussed above. But the computed *B* terms for the L_b and L_a transitions are due almost exclusively to their mutual magnetic mixing, leading to the prediction of large positive and negative *B* terms. The *B* terms predicted by LCOAO for the L_b transitions in benz[*a*]anthracene, chrysene, and BaP are +0.09,[7] +0.11,[5] and +5.1 ($10^{-3}\beta_e D^2/cm^{-1}$), reflecting the predicted increase in hardness and consistent with the observed trend: The experimental values are estimated to +0.1,[7] +0.38,[5] and +1.00.

Summary

The combined information from UV and IR linear dichroism, fluorescence polarization, and MCD spectroscopy and from quantum chemical calculations using several models has lead to a detailed characterization of electronic transitions in BaP. Accurate experimental transition moment directions are determined for the four dominant transitions in the region below 43 000 cm^{-1}. These transitions can be classified as L and B in the perimeter model, and their energies, relative intensities, moment directions, and MCD signs are well reproduced by the LCOAO calculation. According to the theoretical analysis, the perturbation of the alternant pairing symmetry of BaP is unusually large for a benzenoid hydrocarbon. The breakdown of the pairing symmetry is consistent with the observed strong MCD spectrum which corresponds to that of a positive-hard MCD chromophore (ΔHOMO > ΔLUMO).

Acknowledgment. We are grateful to Bengt Nordén for help with the fluorescence polarization experiments, to Josef Michl for the opportunity to use his spectropolarimeter, to Dongni Wang for measuring the LD IR spectrum, to Rolf Gleiter for providing computer time at the Universitätsrechenzentrum in Heidelberg, and to Panther Plast A/S, DK-4760 Vordingborg, for a gift of pure polyethylene. Financial support from the Danish Natural Science Research Council is gratefully acknowledged.

Registry No. Benzo[*a*]pyrene, 50-32-8.

Vibrational Coupling between Ethylidyne Species on Platinum Particles

Dilip K. Paul, Thomas P. Beebe, Jr.,† Kevin J. Uram, and John T. Yates, Jr.*

Contribution from the Surface Science Center, Department of Chemistry, University of Pittsburgh, Pittsburgh, Pennsylvania 15260. *Received August 30, 1991*

Abstract: Vibrational coupling between neighboring ethylidyne species adsorbed on a Pt/Al_2O_3 catalyst has been detected using an equimolar mixture of $^{13}CH_3C(a)$ and $^{12}CH_3C(a)$. The coupling is detected by means of the development of increased intensity sharing in the symmetric C–H deformation mode for the chemisorbed ethylidyne species as the ethylidyne coverage increases. The results indicate that ethylidyne is produced from ethylene on (111) facets of small Pt particles, rather than on random trimer Pt sites which might also exist on the catalyst. Experiments on highly dispersed Pt catalyst surfaces have failed to detect ethylidyne production.

I. Introduction

A. Ethylidyne as a Detector of 3-Fold Metal Atom Sites on Catalytic Surfaces. The interaction of ethylene with the Pt group metal surfaces is of central importance in heterogeneous catalytic chemistry due to the widespread involvement of olefinic molecules in important catalytic processes.[1] Within the last several years, it has been learned that ethylene efficiently converts to the ethylidyne species $CH_3C(a)$ near 250 K on the (111) planes of the fcc Pt group metals, or on the Ru(001) surface.[2-5] Thus, ethylidyne formation is indicative of the presence on single-crystal surfaces of metal atom sites possessing 6-fold symmetry in the upper layer. This is consistent with the sp^3 hybridization of the nonhydrogenic C atom in $CH_3C(a)$. The identification of ethylidyne on the 6-fold symmetric single-crystal planes has been made by vibrational spectroscopy,[6,7] LEED,[8,9] and SIMS studies.[10] In addition to these direct structural methods, the analogy of adsorbed ethylidyne to the ethylidyne moiety in organometallic compounds has been well established.[11]

In addition to work on single-crystal surfaces, several studies have dealt with ethylidyne formation on supported metal catalysts.[12-18] Here, infrared spectroscopy has been the primary tool for study, and the vibrational frequencies observed agree quite well with those found on single-crystal metals and in organometallic compounds. Work on Pd/Al_2O_3 has shown that approximately one-third of the exposed Pd sites are capable of adsorbing CH_3C species[14] and that these species are spectator species to the catalytic hydrogenation of ethylene to produce ethane.[13] Additional investigations of Rh/Al_2O_3, Ru/Al_2O_3, and

†Present address: Department of Chemistry, University of Utah, Salt Lake City, UT 84112.

(1) Horiuti, J.; Miyahara, K. *Hydrogenation of Ethylene on Metallic Catalysts*; Government Printing Office: Washington, DC, 1968; NBS-NSRDS No. 13.
(2) Steininger, H.; Ibach, H.; Lehwald, S. *Surf. Sci.* **1982**, *117*, 685.
(3) Kesmodel, L. L.; Grates, J. A. *Surf. Sci.* **1981**, *111*, L747.
(4) Koel, B. E.; Bent, B. E.; Somorjai, G. A. *Surf. Sci.* **1984**, *146*, 211.
(5) Barteau, M. A.; Broughton, J. Q.; Menzel, D. *Appl. Surf. Sci.* **1984**, *19*, 92.
(6) Ibach, H.; Hopster, H.; Sexton, B. *Appl. Surf. Sci.* **1977**, *1*, 1.
(7) Malik, I. J.; Brubaker, M. E.; Mohsin, S. B.; Trenary, M. *J. Chem. Phys.* **1987**, *87*, 5554.
(8) Kesmodel, L. L.; Baetzold, R. C.; Somorjai, G. A. *Surf. Sci.* **1977**, *66*, 299.
(9) Kesmodel, L. L.; Dubois, L. H.; Somorjai, G. A. *Chem. Phys. Lett.* **1978**, *56*, 267.
(10) Creighton, J. R.; White, J. M. *Surf. Sci.* **1983**, *129*, 327.
(11) Skinner, P.; Howard, M. W.; Oxton, I. A.; Kettle, S. F. A.; Powell, D. B.; Sheppard, N. *J. Chem. Soc., Faraday Trans. 2* **1981**, *77*, 1203.
(12) A more thorough review of these and other ethylidyne studies is given in: Beebe, T. P., Jr.; Albert, M. A.; Yates, J. T., Jr. *J. Catal.* **1985**, *96*, 1.
(13) Beebe, T. P., Jr.; Yates, J. T., Jr. *J. Am. Chem. Soc.* **1986**, *108*, 663.
(14) Beebe, T. P., Jr.; Yates, J. T., Jr. *Surf. Sci.* **1986**, *173*, L606.
(15) Beebe, T. P., Jr.; Yates, J. T., Jr. *J. Phys. Chem.* **1987**, *91*, 254.
(16) Mohsin, S. B.; Trenary, M.; Robota, H. J. *J. Phys. Chem.* **1988**, *92*, 5229.
(17) Sheppard, N.; James, D. I.; Lesiunas, A.; Prentice, J. D. *Commun. Dept. Chem. Bulg. Acad. Sci.* **1984**, *17*, 95.
(18) Lapinski, M. P.; Ekerdt, J. G. *J. Phys. Chem.* **1990**, *94*, 4599.

0002-7863/92/1514-1949$03.00/0

Pt/Al_2O_3 catalysts have all shown that ethylidyne is produced on these surfaces and may be detected by infrared spectroscopy.[15-18] In addition, one study on Pd/Al_2O_3 has shown that, under certain conditions, ethylidyne formation is partially blocked by another adsorbed species produced from ethylene having a binding energy of about 10 kcal/mol.[19]

Prior to the present study it was not known whether, on supported metal catalysts, the metal binding sites of triangular symmetry which are involved in the formation and binding of ethylidyne were generally found in groups such as would be present on an extended (111) facet of a metal catalyst particle or are predominantly on 3-fold metal sites located randomly on the metal particle surface and therefore largely isolated from one another.

We have therefore devised an experiment utilizing a previously observed phenomenon known as adsorbate–adsorbate vibrational coupling, which is able to detect lateral interactions between neighboring adsorbed ethylidyne species. In this experiment, if vibrational coupling is observed, then it is very likely that the ethylidyne species form on 3-fold adsorption sites which are collectively located in groups, as are found on extended (111) facets. On the other hand, if vibrational coupling is not observed, then it is likely that the 3-fold sites on which the ethylidyne species form are not located close to other similar 3-fold sites. From the present work it appears as if the former model for the distribution of 3-fold Pt sites applies and that ethylidyne should be thought of as a detector for the presence of Pt(111) microfacets on Pt catalyst surfaces.

B. Lateral Interactions and Vibrational Coupling. Intermolecular interactions between adsorbed species are of importance in many surface phenomena. Examples include the variation in adsorption energy with adsorbate coverage and the presence of surface phase transformations in the adsorbed layer. Unlike these static forms of lateral interactions, a dynamic form of interaction has recently been proposed to account for the behavior of adsorbed molecules such as CO, which are vibrating on the surface. It has previously been demonstrated for CO adsorbed on a variety of single-crystal surfaces,[20-24] and originally for CO on supported metal surfaces,[25,26] that very large frequency shifts and disparities in intensity ratios for mixed isotopes accompany the increase of CO coverage on these surfaces. Two models have emerged to account for these effects, as outlined below.

The first model, proposed as early as 1956 by Eischens, Francis, and Pliskin,[25,26] described results in which CO molecules adsorbed on Pt particles exhibited a large increase in frequency with coverage, which was attributed to the coupling of dynamic dipoles of the oscillating CO molecules. This lateral, through-space interaction, dipolar coupling, was later expanded upon greatly by Hammaker, Francis, and Eischens in 1965[27] and by others through the intervening years.[28-30] A variety of experimental investigations[20-27] have appeared in addition to the above theoretical model. This model has been criticized by some workers[24,28,31] because of its inability to account for the large frequency shifts sometimes observed experimentally with increasing CO coverage. The dipole coupling model integrates over the many adsorbate–adsorbate interactions, and the magnitude of these interactions decays as r^{-3}.

A second model has emerged which considers fewer adsorbate–adsorbate interactions but which can nevertheless account for experimentally large frequency shifts and intensity disparities with increasing coverage. This model, vibrational coupling, considers only the interactions between nearest-neighbor adsorbates and is a type of through-bond (through-metal) interaction. This model was originally developed by Cotton and Kraihanzel[32] for application to the bonding of multiple CO ligands in metal carbonyl species and was recently adapted by Moskovits and Hulse[31] for the case of CO bonding on metal surfaces. This model argues that there is some overlap between the adjacent adsorbate molecular orbitals. Cotton and Kraihanzel[32] and Moskovits and Hulse[31] argued that as one C–O bond stretches, it causes a change in the adjacent bonding orbitals of its neighbors, which in the simplest of terms can be described as a system of coupled harmonic oscillators.

For example, in eq 1 describing the harmonic potential of two coupled oscillators, there is a cross-term for the interaction of the two coupled oscillators, $k_{12}Q_1Q_2$. In eq 1, k_1 (k_2) is the force

$$V = \tfrac{1}{2}[k_1Q_1^2 + k_2Q_2^2 + k_{12}Q_1Q_2] \quad (1)$$

constant for oscillator 1 (oscillator 2), Q_1 and Q_2 are the displacements from equilibrium bond length of oscillators 1 and 2, respectively, and k_{12} is the coupling force constant. For the case when the masses of the two coupled oscillators are the same (i.e., when the same isotope is employed), the system of two oscillators is described by two normal modes, one in which the adsorbate bonds vibrate in-phase (the "symmetric mode") and one in which the adsorbate bonds vibrate exactly out-of-phase (the "asymmetric mode"). Since the system of two identical isotopes bonded normally on a surface has the same maximum displacement from equilibrium for each oscillator, the asymmetric mode will not produce a net change in dipole moment during execution of this normal mode and consequently is not infrared-active. The symmetric mode, however, is an infrared-active mode. This symmetric vibration is the motion responsible for the observed frequency shifts with increasing coverage of ^{12}CO on a variety of surfaces.[20-27]

When a mixture of two different isotopes is adsorbed on a surface (one ^{13}CO and one ^{12}CO in the two-coupled oscillator example given above) both the in-phase and out-of-phase motions[33] give rise to infrared intensity, since in the out-of-phase motion the different masses lead to a slightly different maximum displacement from equilibrium and, hence, a nonzero net change in dipole moment during execution of the normal mode. Increasing the coverage of such a system of mixed-isotope oscillators would have the equivalent effect, in the prototype example of two oscillators, of increasing the value of k_{12}. This leads to a splitting and repelling of the frequencies (one shifts up while the other shifts down) of the high- and low-frequency modes and an "intensity sharing or borrowing" (the high-frequency mode exhibits more and the low-frequency mode exhibits less intensity than they would for the uncoupled case). In the limit of infinite dilution (zero coupling), the adsorbed oscillators exhibit their singleton frequencies and natural intensities. In this limit of infinite dilution, the intensity ratio may not be exactly unity for the mixed-isotope system since a smaller maximum displacement from equilibrium, and hence a smaller infrared intensity, may be exhibited by the heavier isotope.

Since an excellent review of the vibrational coupling and dipole coupling models has recently been given,[24] we will not review these models in any more depth than what has already been given above, except to describe our methods of calculation in a later section.

Unlike all previous experimental and theoretical work on the subject of dipole or vibrational coupling, which has involved CO

(19) Albert, M. R.; Yates, J. T., Jr. *Surf. Sci.* **1987**, *192*, 225.
(20) Crossley, A.; King, D. A. *Surf. Sci.* **1977**, *68*, 528.
(21) Shigeishi, R. A.; King, D. A. *Surf. Sci.* **1976**, *58*, 379.
(22) Campuzano, J. C.; Greenler, R. G. *Surf. Sci.* **1979**, *83*, 301.
(23) Hollins, P.; Pritchard, J. *Surf. Sci.* **1979**, *89*, 486.
(24) Willis, R. F.; Lucas, A. A.; Mahan, G. D. *The Chemical Physics of Solid Surfaces and Heterogeneous Catalysis*; King, D. A., Woodruff, D. P., Eds.; Vol. 2, pp 67–100.
(25) Eischens, R. P.; Pliskin, W. A. *Adv. Catal.* **1958**, *10*, 1.
(26) Eischens, R. P.; Francis, S. A.; Pliskin, W. A. *J. Phys. Chem.* **1956**, *60*, 194.
(27) Hammaker, R. M.; Francis, S. A.; Eischens, R. P. *Spectrochim. Acta* **1965**, *21*, 1295.
(28) Mahan, G. D.; Lucas, A. A. *J. Chem. Phys.* **1978**, *68*, 1344.
(29) Scheffler, M. *Surf. Sci.* **1979**, *81*, 562.
(30) Sorbello, R. S. *Phys. Rev. B* **1985**, *32*, 6294.
(31) Moskovits, M.; Hulse, J. E. *Surf. Sci.* **1978**, *78*, 397.
(32) Cotton, F. A.; Kraihanzel, C. S. *J. Am. Chem. Soc.* **1962**, *84*, 4432.
(33) More correctly, for the case of the mixed-isotope system, since the uncoupled oscillators do not have the same frequency, an exact in-phase and out-of-phase motion does not exist. However, in analogy to the system of two identical oscillators, a high-frequency system eigenmode exists for the motion which is largely in-phase, and a low-frequency system eigenmode exists for the largely out-of-phase motion. The low-frequency mode, because of the near net cancellation of dipoles, is of much lower intensity than the high frequency mode.

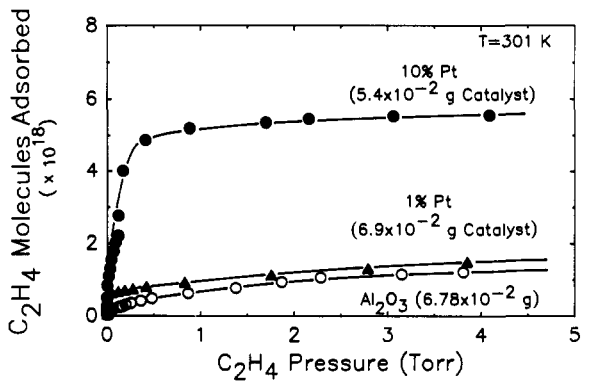

Figure 1. Adsorption isotherm for C_2H_4 on Pt/Al_2O_3 at 301 K.

as the oscillator, the present paper describes results for mixed isotopes of ethylidyne, $CH_3C(a)$, adsorbed on small Pt particles supported on alumina. We have previously reviewed[12] the chemistry of the ethylidyne species and have shown that the isotopic mass of the methyl carbon atom is largely involved in determining the vibrational frequency of the symmetric methyl deformation mode.[13] By using singly labeled ethylene ($^{13}CH_2$=$^{12}CH_2$) as the precursor molecule to ethylidyne species formation, we have, quite naturally, guaranteed that regardless of coverage a statistically equal mixture of $^{12}CH_3C(a)$ and $^{13}CH_3C(a)$ species exists on the surface of our Pt particles. We have modeled our experimental system by a triatomic species, M–X–Y, within the framework of vibrational coupling given previously by Moskovits and Hulse[31] and as described in more detail below.

II. Experimental Methods

Both 10% and 1% Pt/Al_2O_3 catalysts have been studied. The catalysts were prepared using $PtCl_4$ (Alfa Products) which is dissolved in 1 part of H_2O and diluted with 9 parts of acetone. Into this, aluminum oxide (Degussa aluminum oxide C; 100 m^2/g) is dispersed. This slurry was sprayed through an atomizer onto a CaF_2 sample support plate to produce a final density of 10.7 mg/cm^2 for the 10% Pt catalyst and 13.7 mg/cm^2 for the 1% Pt catalyst. The sample plate was mounted inside a stainless steel IR cell[34] which is connected to an ultrahigh-vacuum system containing provisions for pressure measurements in the range 10^{-8}–1000 Torr. The sample was outgassed for 48 h at 475 K and then reduced four times for 15, 30, 45, and 60 min at 475 K using H_2 at 400 Torr. Between each reduction cycle, the sample was evacuated to 10^{-6} Torr for 30 min. The reduced catalyst was then allowed to remain under vacuum at 475 K for a period of 12 h. The reduced Pt/Al_2O_3 catalyst was then cooled under vacuum to ambient temperature and used for the measurements described here.

The reagents used in this study include H_2 (Matheson, 99.995%) and unsymmetrically isotopically labeled $^{13}CH_2$=$^{12}CH_2$, obtained from MSD Isotopes with 99% ^{13}C labeling on the single carbon. Other studies were done with nonenriched C_2H_4 (Matheson, 99.9995% purity).

Spectral measurements were made using a Perkin-Elmer 783 infrared spectrometer coupled to a 3600 data acquisition system operating at a resolution of 2.4 and 5.4 cm^{-1} at 1000 cm^{-1}. For measurements made in the 1340-cm^{-1} region, where detailed spectra of the ^{13}C + ^{12}C labeled $CH_3C(a)$ species were acquired, the resolution employed was 2.4 cm^{-1} and the data acquisition was made at 1 point/cm^{-1} with typical data acquisition times of 52 s/cm^{-1}. No spectral smoothing function was used during manipulation of the data.

Figure 1 shows adsorption isotherms for ethylene on a 10% Pt catalyst, a 1% Pt catalyst, and the Al_2O_3 support. The results obtained from the 10% Pt catalyst may be used to relate the number of C_2H_4 molecules adsorbed to the saturation coverage of C_2H_4 which may be produced on the surface.

The electron micrographs were taken with a Philips 420ST transmission electron microscope, equipped with a top entry stage. The powder sample was ultrasonically dispersed in ethanol, and the suspension was deposited on a copper grid coated with a holey carbon film. The suspension was then air-dried. The magnification of the microscope was 5 × 10^5, and the images were taken in a bright-field mode.[35]

(34) Wang, H. P.; Yates, J. T., Jr. *J. Phys. Chem.* **1984**, *88*, 852.

(35) We thank Dr. Stephen B. Rice and Dr. M. M. J. Treacy for carrying out the TEM studies at the Exxon Research and Engineering Co., Annandale, NJ 08801.

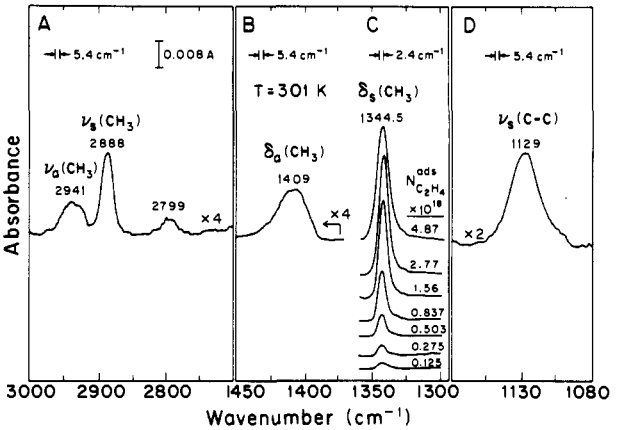

Figure 2. Infrared spectra showing the characteristic vibrational modes of ethylidyne (CH_3C) on Pt/Al_2O_3 at 300 K.

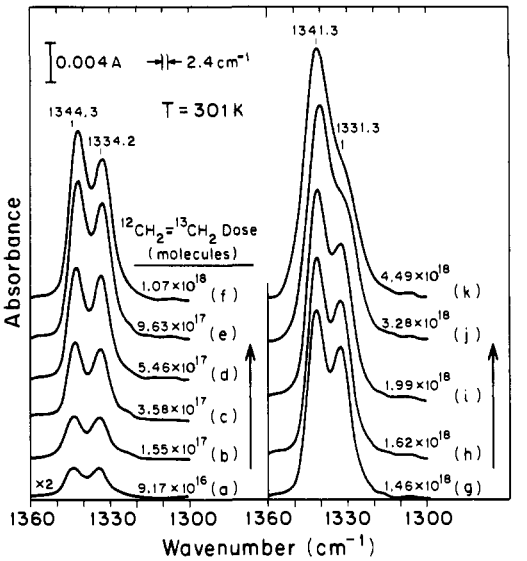

Figure 3. Infrared spectra of $\delta_{sym}(CH_3)$ mode for ethylidyne species produced by adsorbing $^{13}CH_2$=$^{12}CH_2$ on 10% Pt/Al_2O_3.

III. Results

A. Spectroscopic Identification of Ethylidyne Formation on Pt/Al_2O_3. Experiments were first performed using unlabeled C_2H_4 on 10% Pt/Al_2O_3 catalysts at 300 K. Figure 2 shows the spectroscopic developments in three regions of the infrared spectrum corresponding to the vibrational motions of the ethylidyne species. In Figure 2A, the asymmetric (2941-cm^{-1}) and symmetric (2888-cm^{-1}) methyl stretching motions of the $CH_3C(a)$ species are observed. Mohsin et al.[16] have assigned the 2799-cm^{-1} band to the first overtone of the asymmetric methyl deformation mode of ethylidyne. Previous studies[13] have shown that this mode is unrelated to the ethylidyne species. In Figure 2B,C, the asymmetric and symmetric deformation modes for $CH_3C(a)$ are shown, and in the case of the symmetric mode, its development at 1344.5 cm^{-1} is shown as a function of the number of molecules of C_2H_4 adsorbed, $N^{adsorbed}_{C_2H_4}$. It may be seen that, for the isotopically pure $CH_3C(a)$ species, a single $\delta_{sym}(CH_3)$ mode is observed at all coverages. In Figure 2D, the C–C stretching mode for $CH_3C(a)$ is shown at 1129 cm^{-1}. The frequencies of these five modes of ethylidyne are in good agreement with the measurements of others for the ethylidyne species,[6,7,15–17] leaving no doubt regarding their assignment.

B. Mixed-Isotope Studies. Figure 3 shows the spectral development for a series of increasing coverages of the mixed $^{13}CH_3C(a)$ and $^{12}CH_3C(a)$ species on the 10% Pt/Al_2O_3 catalyst. As discussed in the Introduction, the coverage ratio for the two isotopic species is unity for all of these experiments. It is noted that, at the lowest coverages of ethylidyne, the two isotopic species

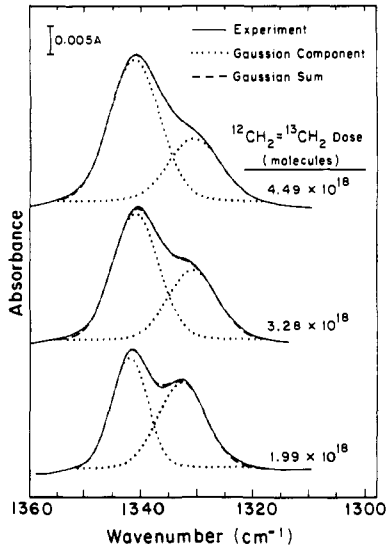

Figure 4. Infrared spectra for the $\delta_{sym}(CH_3)$ mode for an equimolar $^{13}CH_3{}^{12}C$ and $^{12}CH_3{}^{13}C$ mixture at high coverages and their deconvoluted components using a Gaussian fit.

result in two bands separated by about 10 cm^{-1} which exhibit equal integrated intensities and peak heights. As the mixed-isotope ethylidyne layer is increased in coverage by additional ethylene adsorption, the intensity ratio varies systematically, with the higher frequency feature becoming more dominant. At full coverage, spectrum k, the lower-frequency mode can be seen only as an unresolved shoulder on the high-frequency mode.

The two components of the overlapping ethylidyne bands for the mixed-isotope experiments have been deconvoluted into two components using Gaussian fits, and three examples of this procedure are given in Figure 4. An analysis of all of the spectra in Figure 3 involving deconvolution into Gaussian components has shown that over the coverage range studied here downward frequency shifts of ~3 cm^{-1} occur as coverage increases. This *small* shift in the downward direction for the interacting isotopic ethylidyne species is a unique result when compared to previous results for CO adsorbed on various single-crystal surfaces. It is a direct consequence of the vibrational coupling model that if no other effects are operating, relative intensity changes and frequency shifts must both be exhibited with increasing coverage. These effects have been observed, to varying extents, for CO adsorbed on various single-crystal surfaces. That only very small frequency shifts accompany the fairly large change in intensity ratio is evidence that an additional physical effect is occurring here, such that frequency shifts caused by vibrational coupling are offset to a large degree by other physical effects. Hollins and Pritchard[23] have demonstrated that this is the case also for CO isotopes adsorbed on Cu(100). The lack of coverage-dependent frequency shifts for the isotopically pure $^{12}CH_3C(a)$ are observed in Figure 2C, where the maximum shift in δ_{sym} is less than 1.0 cm^{-1} over the full coverage range.

Figure 5 presents a plot of the experimental peak absorbance ratio for the two $\delta_{sym}(CH_3)$ modes obtained for the isotopic ethylidyne mixture as a function of the fractional coverage of ethylidyne on 10% Pt/Al_2O_3. It is seen that the ratio increases from approximately 1 to 2.3 as the coverage increases and as intermolecular interactions build up. This ratio is independent of whether the experimental peak absorbances (at constant frequency) were obtained from the spectra without analysis (Figure 3) or whether the deconvoluted Gaussian components (Figure 4) are measured.

The behavior shown in Figures 3–5 is easily reversed by hydrogenation of the ethylidyne species at 301 K.[13] Figure 6 shows that the intensity ratios exhibit complete reversibility as ethylidyne is systematically removed by sequential hydrogenation steps with increasing H_2 coverage; the absorbance ratio returns to 1 at lowest ethylidyne coverages.

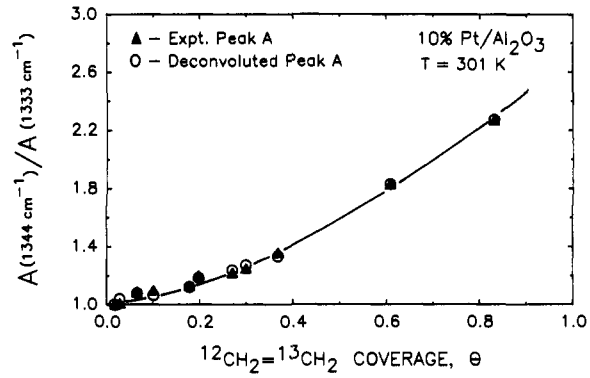

Figure 5. Peak intensity ratio ($A(1344cm^{-1})/A(1333cm^{-1})$) for an isotopic mixture of ethylidyne species as a function of coverage. T = 301 K.

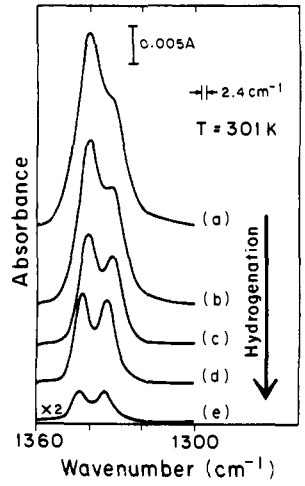

Figure 6. Infrared spectra in the $\delta_{sym}(CH_3)$ region showing the systematic removal of adsorbed ethylidyne species by step-wise $H_2(g)$ addition.

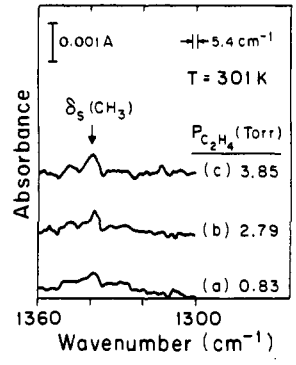

Figure 7. Infrared spectra in the $\delta_{sym}(CH_3)$ region showing an unsuccessful attempt to produce detectable coverages of ethylidyne species on 1% Pt/Al_2O_3 at 301 K.

C. Search for Ethylidyne Formation on Highly Dispersed Pt/Al_2O_3. It is postulated that ethylidyne formation can occur only on Pt sites involving three or more Pt atoms. It would be expected, therefore, that highly dispersed Pt/Al_2O_3 catalysts would be unlikely to form ethylidyne species. This has been verified by studies performed on 1% Pt/Al_2O_3 catalysts. The isotherm measurement (Figure 1) indicates clearly that a very small absolute amount of ethylene is adsorbed on dispersed Pt, and as shown in Figure 7, high-sensitivity spectroscopic studies also show that no $CH_3C(a)$ is formed, at the level of detectability for this species. The sensitivity of the measurement is less than 10% of a saturated monolayer of $CH_3C(a)$, accounting for the different mass of Pt in the 10% and 1% Pt/Al_2O_3 catalysts studied and using the most intense $\delta_{sym}(CH_3)$ spectrum in Figure 2 as a calibration for monolayer intensity.

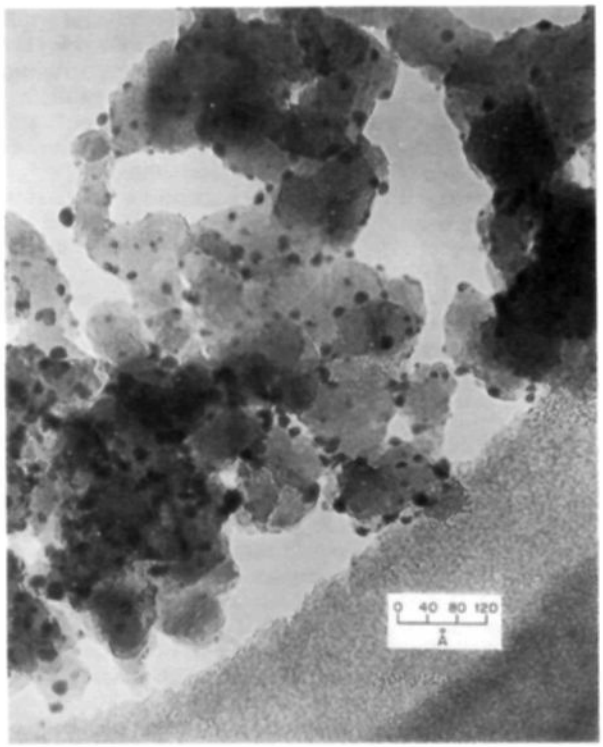

Figure 8. Transmission electron micrograph of a 10% Pt/Al_2O_3 sample. Photograph supplied at scale 1 cm = 40 Å.

D. Transmission Electron Microscopy of Pt/Al_2O_3. Figure 8 shows the electron micrographs of the 10% Pt/Al_2O_3 specimens, showing quite small and well dispersed Pt particles ranging from about 10 to 40 Å in diameter; the average size is about 20 Å. The contrast of small metal particles seen in the transmission electron micrograph (TEM) is strongly dependent upon the orientation of the crystalline Al_2O_3 substrate. Some of the crystallites clearly show faceting, although this is not universally true in the areas examined. Others are less clearly faceted and appear to have rounded surfaces. The morphology of Pt particles is found to be fcc cubo-octahedra with either a (111) or a (110) face in contact with the basal Al_2O_3 plane. The coincidence of (110) type facets with lattice fringes in the alumina suggests the possibility of some sort of expitaxial growth of Pt on the Al_2O_3 support.

IV. Discussion

A. Modeling of Experimental Results. The procedure used to generate the single-isotope and mixed-isotope spectra was identical to the technique described by Moskovits and Hulse,[31] with the exception that the present system was modeled as a surface triatomic species while Moskovits and Hulse used a surface diatomic species. Infrared spectra were simulated by first randomly placing 36 triatomic species, either single isotope or mixed isotope, on an fcc (111) surface. In the case of the mixed-isotope spectra, 18 of each species were randomly placed on the surface. After the adsorption lattice was constructed, the **F** matrix was generated as described by Moskovits and Hulse. Only 36 species were used in these simulations due to the extreme computational effort required to diagonalize the **F** matrix.

Ethylidyne was modeled as a triatomic species which is adsorbed parallel to the surface normal as shown below.

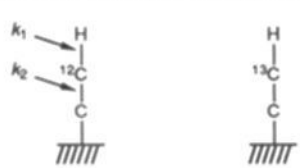

Force constants were then empirically determined by comparing the observed vibrational frequencies for both isotopes with the calculated frequencies. Values for $k_1 = 506$ N m^{-1} (1 N m^{-1} = 10^{-2} mdyn Å^{-1}) and $k_2 = 87.2$ N m^{-1} gave acceptable frequencies for the ^{12}C–H (^{13}C–H) deformation of 1344 cm^{-1} (1333 cm^{-1}) and the ^{12}C–C (^{13}C–C) stretch of 1095 cm^{-1} (1089 cm^{-1}). The experimentally observed values for the above modes, are, respectively, 1344 cm^{-1} (1334 cm^{-1}) and 1129 cm^{-1} (not observed experimentally yet for the ν(^{13}C–C) stretch). In as much as we were able to simultaneously arrive at correct values for both the $\delta_{sym}(CH_3)$ and ν(C–C) modes and to obtain values of the intensity ratio close to those observed experimentally, our approach is in a sense validated by this simultaneous close agreement.

Attempts to model the ethylidyne species with a mass equal to three hydrogen atoms at the top end did not result in acceptable calculated frequencies for either the C–H deformation or the C–C stretching modes. However, the symmetric deformation mode of the methyl group of ethylidyne is amenable to the above triatomic model on the grounds of its symmetry. The motion of the hydrogen atoms can be vector-resolved into a component along the ethylidyne C_3 axis and a component perpendicular to this axis. The latter component is identically zero for the symmetric deformation, while the collective motion of the three hydrogen atoms in the former component can be represented by a single mass moving along the molecule's C_3 axis. The effective mass of this dummy mass is 3 sin (109.54 – 90)° = 1.

The **F** matrix was diagonalized using the method of Jacobi as described by Moskovits and Hulse and programatically outlined by Gorry.[36] At this point, the **F** matrix is simply a diagonalized **F** matrix for the series of oscillators which would yield eigenvalues equal to that of a single oscillator. An anharmonic coupling constant, k_{12}, which couples the motion of the C–H deformation of one ethylidyne species to the C–H deformation of its nearest-neighbor ethylidyne species was introduced. This term gives rise to off-diagonal elements in the **F** matrix and causes the intensity disparity which is observed experimentally.

The value of k_{12} was chosen by an empirical procedure similar to the way in which the primary force constants k_1 and k_2 were chosen. Here, the considerations were 2-fold. We sought to match the experimentally observed maximum intensity ratio and yet produce the smallest shift in frequency with coverage, since only tiny frequency shifts were observed experimentally. However, as discussed above, the vibrational coupling model necessarily produces the concomitant effects of frequency shift and intensity disparity or "intensity sharing", and consequently our calculated spectra indeed show both effects. Our empirically chosen anharmonic coupling constant is 0.2 N m^{-1}.

The results of the above calculation yield a system of 72 eigenfrequencies with corresponding intensities. The spectrum for such a system was simulated by placing a Gaussian-shaped peak of the appropriate height at each of the calculated frequencies and performing a summation over the spectral range of interest. A value of 7.0 cm^{-1} was used for the fwhm of the Gaussian peaks because this is the narrowest fwhm observed for the [^{12}C]-ethylidyne spectrum at full coverage on these surfaces, which is probably due to inhomogeneous broadening.

Figure 9 shows a series of simulated infrared spectra for an equal isotopic mixture of $^{12}CH_3{}^{13}C$ and $^{13}CH_3{}^{12}C$ adsorbed on a Pt surface. The set of infrared spectra presented in Figure 9 is qualitatively similar to the experimental results presented in Figure 3. There is a slight frequency shift of approximately 4 cm^{-1} of the in-phase symmetric deformation mode toward higher frequency with increasing coverage that is not observed in the experimental results. This is a result of the coupling constant in the cross-terms of the **F** matrix. This frequency shift may not be observed experimentally due to competing chemical effects with increasing coverage as is observed for CO chemisorbed on Cu(111).[23]

Figure 10 shows the calculated ratio of the in-phase symmetric deformation intensity with respect to the out-of-phase deformation intensity as a function of coverage. The in-phase and out-of-phase

(36) Gorry, P. A. *Basic Molecular Spectroscopy*; Butterworths: Kent, England, 1985.

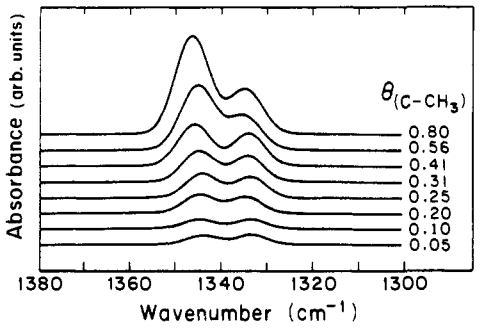

Figure 9. Computed infrared spectra of the $\delta_{sym}(CH_3)$ mode for an equal isotopic mixture of $^{12}CH_3{}^{13}C$ and $^{13}CH_3{}^{12}C$ adsorbed on a Pt surface.

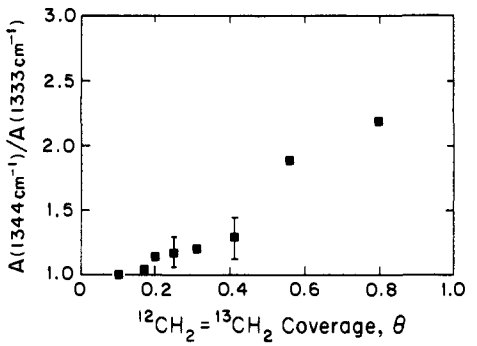

Figure 10. Calculated peak intensity ratio of $\delta_{sym}(CH_3)$ modes (obtained from Figure 9) as a function of ethylidyne coverage.

intensities were defined as the sum of the calculated displacement vectors for modes having frequencies greater than 1339 cm^{-1} and less than 1339 cm^{-1}, respectively. Error bars were determined by calculating the ratio of intensities at a fixed coverage for 10 different random distribution of equal isotopic mixtures of ethylidyne on the surface. The error bars shown in Figure 10 represent the 95% confidence limit on the mean of the absorbance ratio. With such a small sample size (36 oscillators) the largest contribution to the error bars comes from edge effects where coupling is reduced due to reduced nearest neighbor sites.

Figure 10 shows qualitatively similar behavior to the experimental curve of Figure 5. It is worth noting that a single coupling constant gives a good fit to the experimental results throughout the coverage regime. At high coverages, only 45 adsorption sites are required to yield a coverage of $\theta = 0.80$ with 36 oscillators. This suggests that ethylidyne adsorption on facets of very small dimension could produce the observed phenomenon.

B. Implications for the Morphology of Supported Pt on Al_2O_3. This experiment was designed to test whether the principles developed to understand vibrational coupling between adsorbates on single-crystal surfaces can be employed for deeper understanding of species chemisorbed on small metal particles such as those in catalysts. The observation through IR studies of the expected coupling behavior which increases as a function of surface coverage suggests that the Pt particles employed here expose (111) facets which adsorb ethylidyne species as neighbors, permitting vibrational coupling. The results would suggest that an alternate view, involving random arrangements of the majority of Pt atom trimer sites on the 10% Pt catalyst, is unlikely since vibrational coupling between neighbor ethylidyne species would probably be strongly suppressed in this case. This work does not suggest the absence of some isolated Pt_3 sites on 10% Pt/Al_2O_3. Recent XPS and UPS studies of controlled-stoichiometry Pt cluster deposits involving one to six Pt atoms/cluster suggest that with six-atom Pt clusters, metallic behavior is not yet present.[37] This observation is consistent with the assignment in this work of ethylidyne sites as metallic Pt sites having (111) symmetry on small Pt crystallites. Our findings are consistent with conventional views of supported Pt catalyst morphology.

V. Summary

The adsorption of ethylene on a 10% Pt/Al_2O_3 catalyst has been investigated using $^{13}CH_2{=}{}^{12}CH_2$. This isotopic molecule produces an equimolar mixture of $^{13}CH_3C(a)$ and $^{12}CH_3C(a)$ species on trigonal Pt sites. This isotopic mixture permits IR spectroscopy to observe the vibrational coupling between neighboring $CH_3C(a)$ species. Our studies lead to the following conclusions about $CH_3C(a)$ and the Pt sites on which it is produced:

1. Initially, at low coverages, isotopic $CH_3C(a)$ species exist as uncoupled oscillators and exhibit equal IR intensity for the $\delta_{sym}(CH_3)$ mode.
2. As the $CH_3C(a)$ coverage increases, vibrational coupling between neighbor isotopic species leads to intensity sharing, causing the high-frequency coupled mode to increase in intensity relative to the low-frequency mode.
3. A model involving weak intermolecular vibrational coupling of $CH_3C(a)$ species ($\delta_{sym}(CH_3)$mode) successfully predicts the intensity ratio as a function of $CH_3C(a)$ coverage.
4. These coupling observations suggest that $CH_3C(a)$ forms on (111) facets of the Pt particles, rather than on random trimer Pt sites which might also exist on the supported Pt catalyst.
5. Transmission electron micrographs suggest that at least a fraction of the Pt particles are crystalline, exposing (111) facets.
6. This work is an example of the relationship between IR studies on single crystals and on catalysts, where the interplay of concepts derived from the two types of studies is evident.

Acknowledgment. We acknowledge with thanks the support of this work by the Department of Energy, Office of Basic Energy Sciences. We also acknowledge helpful discussions with Professor M. Moskovits. We thank Dr. John Sinfelt of Exxon Research and Engineering for his encouragement of this research project.

Registry No. Pt, 7440-06-4; $H_2C{=}CH_2$, 74-85-1; ethylidyne, 67624-57-1.

(37) Eberhardt, W.; Fayet, P.; Cox, D. M.; Fu, Z.; Kaldor, A.; Sherwood, R.; Sondericker, D. *Phys. Rev. Lett.* **1990**, *64* (7), 780.